ChemComm

Accepted Manuscript

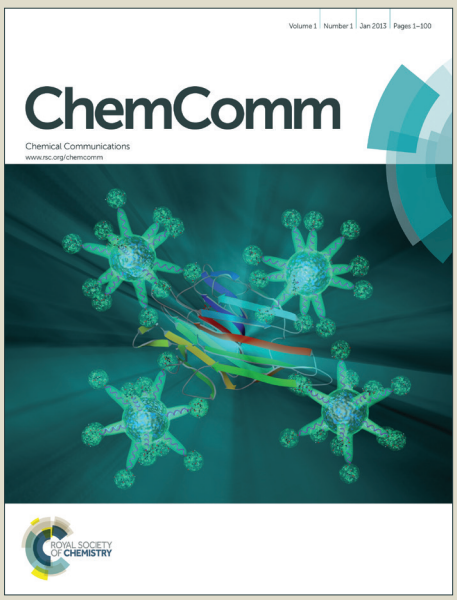

ROYAL SOCIETY OF CHEMISTRY

www.rsc.org/chemcomm

ChemComm

RSCPublishing

COMMUNICATION

www.rsc.org/

Cite this: DOI: 10.1039/xoxxoooooox

Effects of Biomineralization Peptide Topology on the Structure and Catalytic Activity of Pd Nanomaterials

Received ooth January 2012,
Accepted ooth January 2012

DOI: 10.1039/xoxxoooooox

Jose Isagani B. Janairo[a], Tatsuya Sakaguchi[a], Kenji Hara[b], Atsushi Fukuoka[b] and Kazuyasu Sakaguchi[a*]

Highly branched, coral-like Pd nanostructures were formed by a biomineralization peptide conjugated to an oligomeric peptide that simultaneously controls the spatial orientation, arrangement and valency. The Pd nanocoral showed very high catalytic activity in the reduction of nitrophenol. The results highlight the importance of topological arrangement on nanostructure formation and catalytic activity.

Metallic nanomaterials have found increased interest in a wide variety of applications, especially in catalysis due to their enhanced properties over bulk materials. The improvement of catalytic performance of nanomaterials is attributed to the size-dependent and quantum effects.[1] Palladium is very important in catalysis since it is involved in a wide spectrum of reactions, ranging from C-C cross coupling to functional group reductions.[2] Different bottom-up methods can be used to form metal nanostructures, such as the use of stabilizers, templates, and solid supports.[3,4] Among the different techniques of inorganic nanomaterial synthesis, biomineralization is an emerging, bio-inspired method that utilizes biomineralization peptides (BMPep) to modulate the nanostructure.[5] The use of biomineralization peptides offers several advantages over traditional methods of synthesis such as benign conditions, facet binding ability[6] and self-assembly.[7] In addition, biomineralization has been successfully applied in the nanostructure formation of other relevant metals like Pt, Au, Ag and others.[8] Recently, efforts to elucidate factors governing biomineralization have been carried out. From these reports, it has been shown that the BMPep sequence,[9] nature of BMPep binding onto the material surface,[10] BMPep-metal equivalence[11] and buffer type[12] can affect the structure and catalytic activity of nanomaterials formed from biomineralization. It has also been reported that the structure of the BMPep acting as a scaffold can also affect the nanostructure and catalytic activity of the biomineralization products.[13] Therefore, if the spatial orientation, arrangement and valency of the BMPep can be simultaneously defined, this may have a tremendous impact not only on the resulting nanostructure but also with the catalytic performance of the materials. Thus, we examined the effects of defining the topological properties and valency of the BMPep on the structure and catalytic activity of Pd nanomaterials.

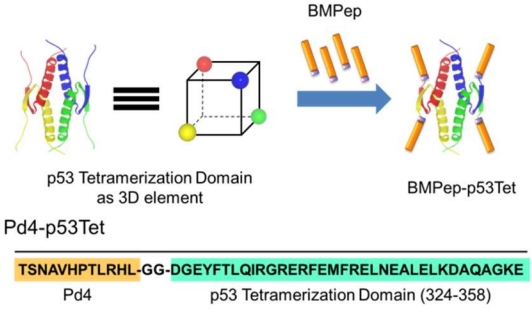

Figure 1. Design strategy of a fusion biomineralization peptide with a highly defined three dimensional orientation. The fusion peptide is composed of a BMPep conjugated with a 3D element. The BMPep used is the Pd4 peptide and the 3D element is the p53 tetramerization domain

Our strategy involves the fusion of a BMPep to a three-dimensional (3D) control peptide. The resulting fusion peptide can simultaneously support the growth of palladium as well as precisely assemble into a well-defined three-dimensional framework; wherein the BMPep spatial orientation and arrangement are specifically assigned. Porous, hierarchical architecture characterized as coral-like materials were obtained using our designed peptide, which possessed superior catalytic performance in the reduction of nitrophenol isomers. Our results highlight the importance of valency and topological arrangement for the BMPep on nanostructure formation and catalytic activity.

The control of valency and topological arrangement for the BMPep was achieved through our designed peptide, Pd4-p53Tet. It is composed of the Pd4 BMPep conjugated to the N-terminus of the tetramerization domain of the tumor suppressor protein p53 (residues 319-356 of human p53). The Pd4 peptide was identified using a phage display assay and can bind to Pd.[14] The Pd4 BMPep has been reported to produce dispersed Pd nanoparticles in buffer-free conditions and at peptide: Pd ratios ranging from 1-4.[15] The Pd4 BMPep modulates nanostructure growth through a capping

[a] Department of Chemistry, Faculty of Science, Hokkaido University, N10 W8, Kita-ku, Sapporo 060-080, Japan.

Email: kazuyasu@sci.hokudai.ac.jp

[b] Catalysis Research Center, Hokkaido University, N21 W10, Kita-ku, Sapporo 001-0021, Japan

†Electronic Supplementary Information (ESI) available: Detailed experimental procedure, EDX elemental mapping, and catalytic data. See DOI: 10.1039/c000000x/

mechanism.[16] The p53 tetramerization domain (p53Tet) on the other hand, is one of the five domains of the tumor suppressor p53 protein. The p53Tet is located at the C-terminal region and each monomer within the tetrameric assembly contains a β-strand (residues 326-333), a tight turn (residue 334), and an α-helix (residue 335-356). Two dimers are formed through the formation of a joint antiparallel β-sheet between monomers, and the two primary dimers tetramerize through hydrophobic interactions of the helices in a four-helix bundle.[17] The p53Tet was chosen as the 3D control element since the positions of the four N-termini in the tetrameric assembly are reminiscent of the vertices of a tetrahedron, which is the simplest 3D object (Fig. 1). The orientation of the N-termini of p53Tet prevents the Pd4 peptides from clashing and interacting with each other while still maintaining a 3D geometry. As a control, the Pd4 BMPep was similarly conjugated to a variant of p53Tet that cannot oligomerize. This monomeric variant of the p53Tet (p53Mono) consists of three alanine substitutions (L330A, I332A and L344A).[18] The Ala substitutions only alter the oligomerization property of the peptide and do not affect the other properties since there is no change in the number and type of functional groups of the peptide. Other control peptides include both the native Pd4 and p53Tet sequences

The respective secondary structures of the synthesized peptides were evaluated by circular dichroism (CD) spectroscopy (Fig. 2).

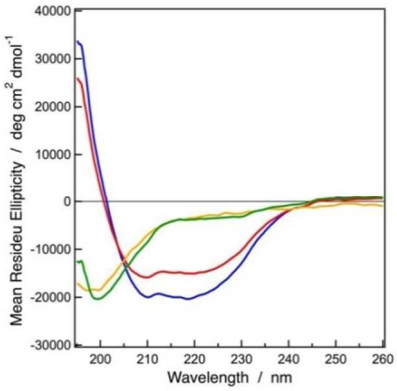

Figure 2. CD spectra for the synthesized peptides. Red = Pd4-p53Tet; Blue = p53Tet; Orange = Pd4; Green = Pd4-p53Mono

The CD spectral profile of Pd4-p53Tet and p53Tet are very similar as expected. This indicates that the Pd4-p53Tet successfully formed tetramers in a similar manner as the native p53Tet and that the Pd4 peptide primarily adopted a random coiled structure. The Pd4-p53Mono peptide likewise exhibited a random coiled structure. This means that Pd4-p53Mono did not form oligomers (ESI, Table S2). Biomineralization was conducted by dissolving the peptides in a HEPES buffered solution (2.5 mM, pH 7.4) to yield a final concentration of 40 μM of the monomer. A five-fold molar equivalence of K_2PdCl_4 (200 μM) was added and after 45 minutes, an excess amount of $NaBH_4$ was added. Reduction was allowed to proceed for 90 minutes at room temperature and the resulting materials were purified by centrifugation. The Pd4-p53Tet facilitated the formation of coral-like Pd structures. These nanostructures are porous which arises from a network of branched filaments (Fig. 3A). This porous characteristic is different from the spherical nanostructures commonly obtained with other biomimetic methods.[11] The absence of lattice lines from TEM images in addition to the halo-like selected area electron diffraction patterns taken at multiple areas indicate that the structures are amorphous (Fig. 3B). EDX elemental mapping (ESI-Fig. S1) confirmed that the structures contain Pd. Moreover, the observed carbon and nitrogen signals indicate the incorporation of the peptide template within the Pd nanostructures. The wide distribution of Pd4-p53Tet within the materials possibly explains the amorphous nature of the Pd structures. The Pd4-p53Tet integrates with the material and prevents the Pd atoms from reorganizing into ordered crystalline structures.[19]

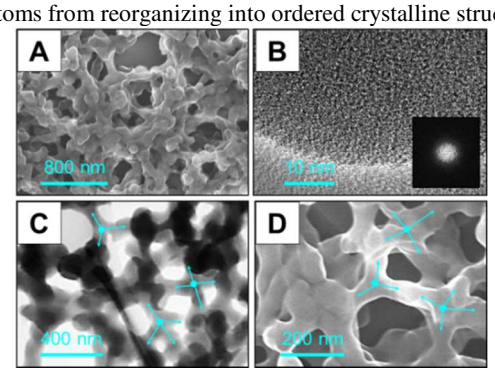

Figure 3. Representative electron microscopy images of the coral-like Pd structures derived from the Pd4-p53Tet peptide. **A**) SE-STEM image showing the porous nature of the Pd structures which emanates from the branched network of filaments. **B**) HRTEM image focusing on a section of the filament which shows the absence of lattice lines. Inset is the SAED FFT pattern confirming its amorphous nature. **C-D**) STEM images showing the tetrahedral orientation of the filaments at different angles.

It was also commonly observed that the Pd4-p53Tet derived nanostructures had several filaments at the pore junction oriented in a tetrahedral orientation (Fig. 3C-D). The tetrahedral arrangement stems from the fact that the Pd4 peptide is fused to the spatially-fixed N-termini of the p53Tet and this validates the rationale for the design of the Pd4-p53Tet. This geometric occurrence is a consequence of the controlled oligomerization through the p53Tet.

Comparative structural analysis was performed with peptide-free, the native Pd4 sequence, the p53Tet and Pd4-p53Mono conditions as negative controls (Fig. 4, Table 1).

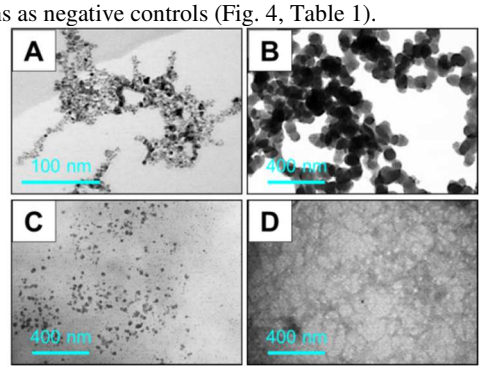

Figure 4. BF-STEM images of Pd nanostructures prepared in the absence or presence of various peptide sequences. A) No peptide, B) Pd4, C) p53Tet, D) Pd4-p53Mono

Small, aggregated particles were formed in the absence of a peptide. The Pd4 BMPep produced globular aggregates of Pd that resembled solid chains. The p53Tet peptide on the other hand, aided the formation of small and dispersed nanoparticles that were irregularly shaped. Finally, a porous thin film which lacked a well-defined and distinct 3D structure was observed from Pd4-p53Mono. The comparative analyses reveal that the coral-like appearance, in addition to the tetrahedral spatial arrangement of the filaments, are exclusively observed for the designed Pd4-p53Tet peptide. The nanocorals were different from the linearly arranged Pd nanoparticles formed using other BMPep in terms of the structure, size and shape.[20] Furthermore, the 3D branched morphology of the nanocorals were different from the nanostructures obtained from other reported fusion BMPep. To name a few examples, Au nanoparticle double helices were formed when dodecanoic acid was used as the control element in which the Au BMPep was attached.[21]

Table 1. Shape, size and catalytic data of the Pd nanomaterials formed from different BMPep for the reduction of nitrophenol isomers.

		Turnover Frequency (h^{-1}) (Pseudo-first order rate constants (k, $x10^{-3}$ s^{-1}))		
	Shape and size	2-nitrophenol	3-nitrophenol	4-nitrophenol
Pd4-p53Tet	Porous, coral-like with 3D network (Filament thickness =104 ± 21 nm)	2390 ± 440 (3.10 ± 0.20)	6650 ± 300 (9.37 ± 0.74)	6510 ± 300 (8.63 ± 0.06)
Pd4	Fused, globular particles (Particle diameter =75.3 ± 9 nm)	600 ± 10 (2.70 ± 0.10)	5640 ± 290 (6.53 ± 0.50)	3150 ± 90 (2.7 ± 0)
Pd4-p53Mono	Network of thin filaments (Filament thickness =28.5 ± 10 nm)	1580 ± 120 (2.4 ± 0.10)	2740 ± 270 (6.83 ± 0.45)	3020 ± 60 (4.13 ± 0.12)
No Peptide	Severely aggregated small particles (Particle diameter =2.86 ± 0.62 nm)	1660 ± 100 (1.97 ± 0.06)	2930 ± 410 (4.07 ± 0.85)	4170 ± 460 (4.23 ± 0.21)
p53Tet	Irregularly shaped and sized dispersed particles (Particle diameter =14.4 ± 9 nm)	2500 ± 120 (3.83 ± 0.06)	7100 ± 240 (7.30 ± 0.10)	4990 ± 130 (7.13 ± 0.06)

Average size was determined from a minimum of 100 measurements. Numbers in parenthesis correspond to the pseudo-first order rate constants. Numbers above the rate constants are the TOF. Conditions: [Substrate] =50 μM, [Pd] =0.8 mol%, [$NaBH_4$] =10 mM, 25^{0}C, triplicate analyses. For detailed procedure, see ESI.

Spherical and rod-like morphologies of Ag were formed when different silk protein sequences were conjugated to Ag BMPep.[22] When a variant of the cowpea virus was used as the control element for Au BMPep, spherical arrangement of Au nanoparticles resembling the shape of the capsid of the virus was observed.[23] Pd4-p53Tet facilitates nanocoral formation through the combined action of both peptide segments within the Pd4-p53Tet fusion. The nanocoral formation follows a multi-step process. Additional experiment revealed that the 45 minute-incubation period of the peptide with Pd ions prior to reduction is necessary to obtain the 3D porous structure. When the incubation period was omitted and reduction was immediately done, flat structures with visibly less porosity were formed (ESI-Fig. S2). This suggests that hierarchical nanostructure formation does not proceed spontaneously and involves multiples steps. The pre-reduction incubation period may be necessary in order for the Pd4-p53Tet to properly assemble. Therefore, it is highly plausible that the Pd nanocoral formation with Pd4-p53Tet proceeds through the following stages (ESI-Fig. S3). The Pd4-p53Tet monomers assemble into a tetramer followed by nanostructure growth at the four Pd4 domains that are spatially-fixed and continues to grow until it is terminated by the linking together of similar units.

The catalytic performance of the formed Pd nanostructures was evaluated using the reduction of nitrophenol to aminophenol as the model reaction. $NaBH_4$ is the reducing reagent wherein a large excess of it in the reaction justifies the use of the integrated rate law ($\ln C_t = -kt + \ln C_0$) for a first order reaction. The rate constant corresponds to the slope of the graph in which $\ln C_t$ was plotted as a function of time. The nanocorals exhibited high catalytic efficiency on the basis of the higher turnover frequency (TOF) for the three different substrates compared from those reported in literature.[24-26] The Pd4-p53Tet nanocorals possessed much higher activity than the materials from Pd4 and Pd4-p53Mono with respect to the TOF and rate constants (Table 1). The superior catalytic performance of the nanocorals can be attributed to the unique 3D branched structure, defined by a high degree of filament cross-links in different directions. The 3D structure of the materials can influence reactivity.[11] On the other hand, the structures from Pd4 and Pd4-p53Mono share the linked morphological feature with the nanocorals but obviously had less 3D character. Comparing the activities of the materials from Pd4-bearing sequence suggests that increasing the 3D character of the material can lead to the formation of high-performance materials. The nanoparticles from peptide-free conditions showed low activity, most likely due to the aggregation of the particles. In contrast were the p53Tet-derived materials which had high catalytic activity. The high activity can be attributed to the small and dispersed nature of the particles which commonly result to favorable catalytic properties such as alteration of the electronic properties, high surface area, among others.[27] Comparing the activities of Pd4-p53Tet and p53Tet raises an interesting observation. The nanocorals were very active despite their larger size. This strongly suggests that the materials with a highly defined 3D structure could give rise to the formation of excellent catalysts. Assigning the topological properties of the BMPep therefore affects not only the nanostructure but the catalytic properties as well. This highlights the importance of specifying the 3D property of the template since the 3D structure of the material depends on it, which influences the catalytic activity. This information expands the knowledge on other known factors that can influence the nanostructure and the catalytic properties of nanocatalysts formed from biomineralization such as the BMPep sequence,[9] nature of the BMPep adsorbed on to the nanomaterial surface[10] and metal salt equivalence.[11]

In summary, we have shown that the precise assignment of the spatial orientation, arrangement and valency of a BMPep can have a significant impact on the resulting nanostructures and their corresponding catalytic performance. The precise topological assignment was achieved through conjugating a BMPep with a 3D control element that can precisely oligomerize into well-defined frameworks. The designed peptide, Pd4-p53Tet yielded Pd nanocorals with high catalytic activity for the reduction of nitrophenol. The high activity of the nanocorals possibly emanates from the high 3D character of the materials. Our study brings forward the possibility that high-performance materials can be formed by using a 3D-controlled template in order to create materials with well-defined 3D structures. Further studies are still however required to fully elucidate the mechanism behind the formation process; as well as determine the behavior of the material

towards the substrates for catalysis. Nonetheless our study expands the existing notion about the factors that affect the nanostructure and catalytic activity of materials formed from biomineralization, such as the BMPep sequence and metal stoichiometry. In addition, our method exhibits both generality and versatility since other BMPep may be similarly conjugated with the p53Tet thus providing a very flexible method for biomineralization control that can be fine-tuned by choosing a specific BMPep.

This work was supported in part by Grant-in-aid for Scientific Research (B) (No. 24310152) from JSPS (to K.S.), Research Fellowships of the Japan Society for the Promotion of Science for Young Scientists from JSPS (No. 24-2657) (to T.S.) and a research grant from the Clark Memorial Foundation at Hokkaido University (to J.I.B.J)

Notes and references

1. E. Roudner, *Chem. Soc. Rev*. 2006, **35**, 583.
2. J. Tsuji, *Palladium Reagents and Catalysts*, John Wiley & Sons: UK, 2004
3. A. Fihri, M. Bouhrara, B. Nekoueishahraki, J.M. Basset, V. Polshettiwar, *Chem. Soc. Rev*. 2011, **40**, 5181.
4. D. Astruc, F. Lu, J.R. Aranzaes, *Angew. Chem. Int. Ed.* 2005, **44**, 7852.
5. F. Nudelman, N. A. J. M. Sommerdijk, *Angew. Chem. Int. Ed.* 2012, **51**, 6582.
6. C-Y. Chiu, Y. Li, L. Ruan, X. Ye, C.B. Murray, *Nat. Chem.* 2011, **3**, 393.
7. C.L. Chen, N.L. Rosi, *Angew. Chem. Int. Ed.* 2010, **49**, 1924.
8. M.B. Dickerson, K.H. Sandhage, R.R. Naik, *Chem. Rev*. 2008, **108**, 4935.
9. R. Coppage, J. M. Slocik, M. Sethi, D.B. Pacardo, R.R Naik, M.R. Knecht, *Angew. Chem. Int. Ed.* 2010, **49**,3767.
10. Y. Li, Z. Tang, P.N. Prasad, M.R. Knecht, M.T. Swihart, *Nanoscale*. 2014, **6**, 3165.
11. R. Bhandari, M.R. Knecht, *ACS Catal.* 2011, **1**, 89.
12. J.I.B. Janairo, K. Sakaguchi, *Chem. Lett.* 2014, DOI: 10.1246/cl.140405
13. R. Bhandari, M.R. Knecht, *Langmuir*. 2012, **28**, 8110.
14. D.B. Pacardo, M. Sethi, S.E. Jones, R.R. Naik, M.R. Knecht, *ACS Nano*. 2009, **3**, 1288.
15. R. Coppage, J.M. Slocik, B.D. Briggs, A.I. Frenkel, R.R. Naik, M.R. Knecht, *ACS Nano.* 2012, **6**, 1625.
16. R. Coppage, J.M. Slocik, B.D. Briggs, A.I. Frenkel, H. Heinz, R.R. Naik, M.R. Knecht, *J. Am. Chem. Soc*. 2011, **133**, 12346.
17. G. M. Clore, J. Ernst. R. Clubb, J.G. Omichinski, W.M.P. Kennedy, K. Sakaguchi, E. Appella, A.M. Groneborn, *Nat. Struct. Biol.* 1995, **2**, 321.
18. R. Kamada, T. Nomura, C.W. Anderson, K. Sakaguchi, *J. Biol. Chem.* 2011, **286**, 252.
19. C.H. Lu, F.C. Chang, F. *ACS Catal.* 2011, **1**, 481.
20. A. Jakhmola, R. Bhandari, D.B. Pacardo, M.R. Knecht, *J. Mater. Chem.* 2010, **20**, 1522.
21. C-L. Chen, P. Zhang, N.L. Rosi, *J. Am. Chem. Soc.* 2008, **130**, 13555.
22. H.A. Currie, O. Deschaume, R.R. Naik, C.C. Perry, D.L. Kaplan, *Adv. Funct. Mater.* 2011, **21**, 2889.
23. J.M. Slocik, R.R. Naik, M.O. Stone, D.W. Wright, *J. Mater. Chem.* 2005, **15**, 749.
24. J. Li, X.Y. Shi, Y.Y. Bi, J.F. Wei, Z.G. Chen, Z-G. *ACS Catal*. 2011, **1**, 657.
25. Q. Wang, W. Jia, B. Liu, A. Dong, X. Gong, C. Li, P. Jing, Y. Li, G. Xu, J. Zhang, *J. Mater. Chem. A.* 2013, **1**, 12732.
26. X. Wu, C. Lu, W. Zhang, G. Yuan, R. Xiong, X. Zhang, *J. Mater. Chem. A.* 2013, **1**,8645.
27. J.D. Aiken III, R.G. Finke, *J. Mol. Catal. A: Chem*, 1999, **145**, 1.

